ANTENNA DESIGN FOR ELECTROMAGNETIC WAVES PROPAGATION STUDIES THROUGH THE SALT ORE

Valeriu SAVU[1], Ion MARGHESCU[2], Octavian FRATU[3], Simona HALUNGA[4], Alina-Mihaela BĂDESCU[5]

Experimental analysis of dielectric properties of the salt and electromagnetic wave propagation trough salt ore can provide opportunities for a small astronomical observatory in a salt mine in Romania. Cherenkov radiation (generated by neutrinos) detection threshold is very low for the salt, and represents half of the ice one. Electromagnetic waves propagation is influenced by salt dielectric parameters (the relative permittivity and tangent loss angle). To select and measure the effects of neutrinos passing through the salt ore, electromagnetic measurements should be conducted under a very low level of radiations, like in the underground case.

Keywords: adaptation, antenna, analyzer, circuit, frequency, salt

1. Introduction

To study the radio emission as a component of very high energy particle radiation from stars, galaxies, quasars, and other astronomical objects which have wavelengths in the range 10 meters (30 MHz) to 1 millimetre (300 GHz) one has to study the shape and the amplitude of pulses generated by the radiation in contact with the earth's atmosphere.

Detection of cosmic radiation with energies greater than $10^{19.5}$ eV implies the existence a neutrino energy flux with energies in the range 10^{17}-10^{19} eV [1].

Generation of radiation pulses that arise from interaction between high energy neutrinos (Ultra High Energy, UHE) and a dense dielectric medium has been first studied by Askaryan [2], who also presented the first results based on laboratory tests.

[1] PhD Student, Faculty of Electronics, Telecommunications and Information Technology, University POLITEHNICA of Bucharest, Romania, e-mail: savuv@inoe.ro
[2] Prof., Faculty of Electronics, Telecommunications and Information Technology, University POLITEHNICA of Bucharest, Romania, e-mail: marion@comm.pub.ro
[3] Prof., Faculty of Electronics, Telecommunications and Information Technology, University POLITEHNICA of Bucharest, Romania, e-mail: ofratu@elcom.pub.ro
[4] Prof., Faculty of Electronics, Telecommunications and Information Technology, University POLITEHNICA of Bucharest, Romania, e-mail: simona_halunga@yahoo.com
[5] Assist., Faculty of Electronics, Telecommunications and Information Technology, University POLITEHNICA of Bucharest, Romania, e-mail: alinabadescu@radio.pub.ro

Askaryan also identified several natural materials that can be used as neutrinos detectors: the salt blocks present in saline mines, the ice from polar region and the soil of moon [3], [4]. It was proven that a solid block of salt is a very good candidate for such detectors, since it suffers important changes of its electrical properties, based on which, the neutrinos that pass through the block can be detected.

Based on the Askaryan effect [5], [6], [7] the radiation that pass through a dense dielectric generates a cone of coherent radiation in the radio or microwave frequency domain, known as Cherenkov radiation [8], [9], [10]. In order to detect this radiation, one has to determine the frequency domain in which those radio impulses have maximum intensity and the parameters of an antenna that can be used in a conventional receiver.

In an experimental setup with a particular configuration of transmitter and receiver antennas one can measure the level and the range of the radiation generated and, based on those results, can evaluate the neutrinos energy. The system proposed in this paper consists in an Anritsu MS2690A signal analyzer, having a signal generator incorporated, coupled to the transmitting and receiving antennas [11].

The reminder of the article is organized as follows. In section two are presented the parameters of the antennas especially developed for the salt mine development. In section three is presented the system setup and the most relevant experimental results, and in section 4 several conclusions and opened issues are highlighted.

2. Design of the system and development details

For the experiments developed in the salt mine, two antennas, centred around 450 MHz and 750 MHz has been especially designed. The main parameters of the antennas as presented in the next section.

2.1. The antennas design

The length of a half-wave (λ/2) dipole antenna is given by [12]:

$$L_{a[\lambda/2]} = \frac{c}{2f\sqrt{\varepsilon_r}} \text{[m]}, \tag{1}$$

where: $c = 3 \times 10^8$ m/s and f is resonance frequency of the antenna [Hz] and ε_r is the electrical permittivity of the transmission media.

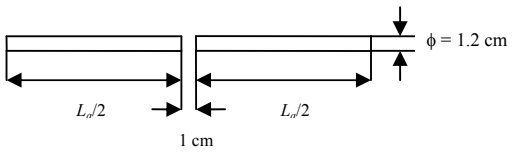

Fig. 1. The half-wave antenna.

For antennas made of copper pipes considering as dielectric the salt, results:

- $L_a = 0.136$ m for $f = 450$ MHz ,
- $L_a = 0.082$ m for $f = 750$ MHz.

The radiation resistance that can be evaluated using [12]:

$$R_{a\,salt} = \frac{2\pi}{3\sqrt{\varepsilon_{r\,salt}}} Z_0 \left(\frac{L_a}{\lambda}\right)^2, \tag{2}$$

where: $\varepsilon_{r\ salt} \approx 6$, $Z_0 = 377\Omega$ and $\lambda = \frac{c}{f}$.

In the specific cases developed, it results:

$$R_{a\,salt\,450MHz} = \frac{1}{\sqrt{6}} 789.587 \left(\frac{0.136}{0.667}\right)^2 = 13.401\ \Omega \text{ for } f = 450 \text{ MHz};$$

$$R_{a\,salt\,750MHz} = \frac{1}{\sqrt{6}} 789.587 \left(\frac{0.082}{0.400}\right)^2 = 13.546\ \Omega \text{ for } f = 750 \text{ MHz}.$$

To match the antennas resistance with the coaxial cable impedance (50Ω) transmission line transformers (balloon) were used. They were built using small ferrite cores in toroidal shapes. The system allows coupling a coaxial cable with a symmetrical antenna (symmetrising circuit). The schematic diagram of the antenna and the matching/symmetrising circuit is shown in Fig. 2.

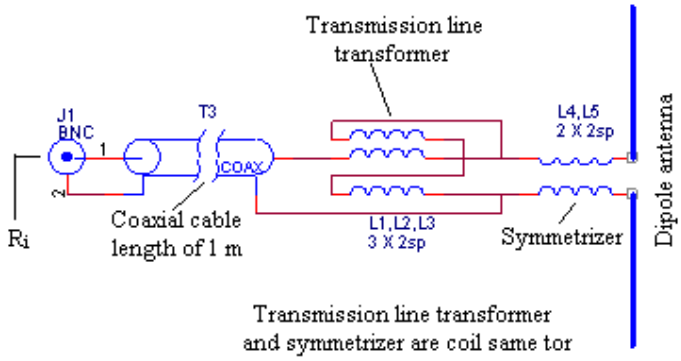

Fig. 2. The schematic diagram of the antennas, including the symmetrising circuitry

The transformation ratio is 1:1 for the symmetrical transformer and 9:4 for the transformer transmission line, so the antenna resistance, measured at the input gate, results as:

- $R_i = 30.152\ \Omega$ for $f = 450$ MHz
- $R_i = 30.478\ \Omega$ for $f = 750$ MHz.

The radiation diagram of the λ/2 dipole antenna is shown in Fig. 3.

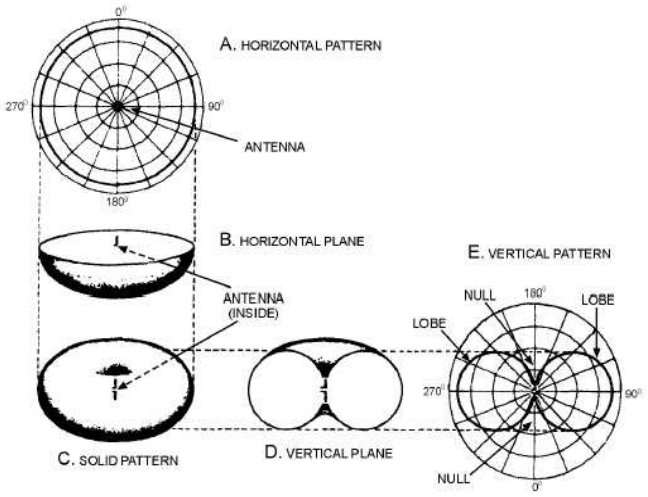

Fig. 3. The radiation diagram for a λ/2 dipole antenna.

To adjust the antenna impedance to a 50 Ω coaxial cable, (type CFD400), a Π matching network was used. The parameters of the matching network, based on [13], are

$$X_2 = \frac{R_s}{\sqrt{\frac{R_s}{R_{sn}}\left(1+Q^2\right)-1}};\ X_2 = \frac{1}{\omega C_2}; \tag{3}$$

$$X_L = \frac{QR_{sn}}{1+Q^2}\left[1+\frac{1}{Q}\sqrt{\frac{R_s}{R_{sn}}\left(1+Q^2\right)-1}\right];\ X_L = \omega L; \tag{4}$$

$$X_1 = \frac{R_{sn}X_G}{QX_G - R_{sn}};\ X_1 = \frac{1}{\omega C_1}; \tag{5}$$

$$Q = \frac{R_{sn}}{\omega L_{ech}}; \tag{6}$$

$$X_G = \frac{1}{\omega C_g}; \tag{7}$$

where:

- R_s is load resistance of the matching circuit, which is the input impedance of the antenna,
- R_{sn} is resistance seen at the adapter output (i.e. the resistance seen by the signal generator of the MS2690A Anritsu analyzer),
- Q is the quality factor of the loaded Π matching circuit,
- $\omega = 2\pi f$ is pulsation of the working frequency,
- C_g is the output capacitance of the MS2690A Anritsu analyzer.

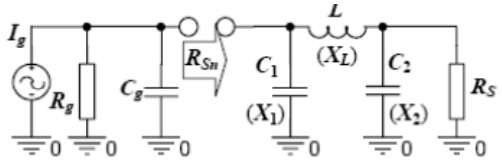

Fig. 4. The Π matching circuit [12].

For the working frequency f = 450 MHz it is known that R_s = 30.152 Ω; R_{sn} = 50 Ω; C_g = 0.1 pF; L_{ech} = 17.18 nH, and, based on relations (3-7) we obtain:

Q = 0.936; X_G = 3536.78 Ω; C_1 = 5.93 pF; C_2 = 387 pF; L = 11.13 nH.

The inductance of the Π matching circuit is given by [14]:

$$L = 200 \cdot l \cdot \left[\ln\left(\frac{4l}{d}\right) - 1 \right] \cdot 10^{-9} \ [H]; \tag{8}$$

where: l is the length of the inductance [m],

d is the diameter of the inductance [m].

To implement the inductance L = 11.13 nH a copper conductor of 17 mm long and with a diameter of 2 mm has been used.

For the frequency f = 750 MHz (see Fig. 6b) we have: R_s = 30.478 Ω, R_{sn} = 50 Ω; C_g = 0.1 pF; L_{ech} = 9.14 nH and we obtained the next values:

Q = 1.116; X_G = 2040.45 Ω; C_1 = 4.45 pF; C_2 = 4.04 pF; L = 7.8 nH,

The schematic diagram for the matching circuit for the two frequencies is shown in Fig. 5.

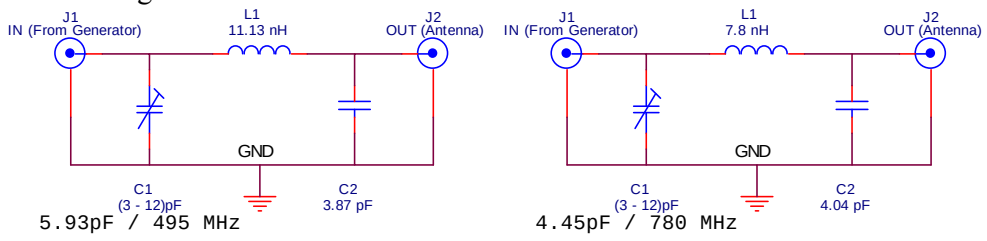

(a) (b)

Fig. 5. Schematic diagram of the Π matching circuit for frequency 450MHz (a), respectively 750 MHz (b).

To implement the inductance L = 7.8 nH, again, a copper conductor with a diameter of 2 mm and 12 mm length has been used.

Fig. 6 shows the physical implementation of the matching circuits designed above.

Fig. 6. Physical implementation of the Π matching circuits for the frequencies of 450 MHz, left and 750 MHz, right.

2.2. Antennas and related circuits implementation

In order to use the antennas in a very corrosive salty environment, an insulator with the shape and dimensions given in Fig. 7 have been developed and inserted between the two dipole elements.

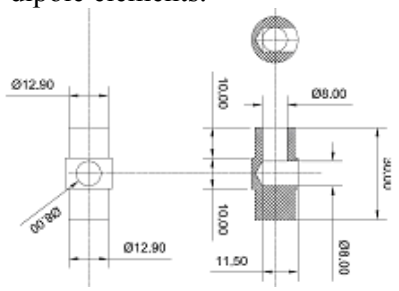

Fig. 7. The insulator dimensions.

For antenna feeding, an RG58LL shielded cable has been used, having a loss of 0.328 dB/m at 400 MHz and 0.459 dB/m at 700 MHz.

The dipole antennas were made of copper pipe with 12mm diameter (Fig. 1). The physical implementation of the antennas and their final implementation using a protection tube are shown in Figs. 8.

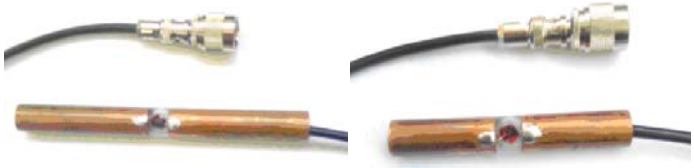

Fig.8a. Antennas for 450 MHz and 750 MHz.

Fig. 8b. Antennas for 450 MHz and for 750 MHz with thermo-contraction protection tube.

Fig. 9 presents the physical implementation of the antennas coupled to the Π matching circuits for the two working frequencies: 450 MHz and 750 MHz.

Fig. 9. Coupling the antenna with the Π matching circuit for frequency 450 MHz, left and 750MHz, right.

In order to adjust the MS2690A Anritsu analyzer with the antenna, an unmodulated signal with a power of 0 dBm produced by the generator block of MS2690A analyzer platform is injected, and, by tuning the trimmer C1, we tried to obtain a maximum value of the signal displayed on the analyser screen, as shown in Fig. 10.

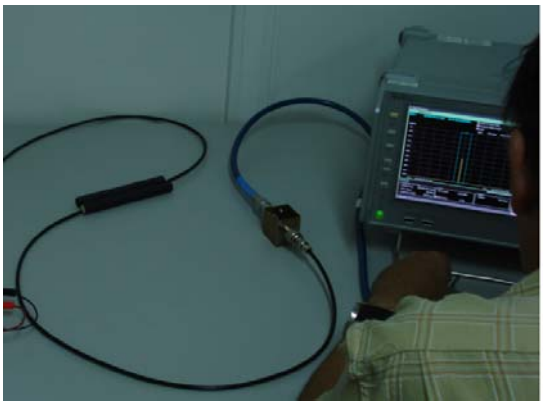

Fig. 10. The test assembly used for the Π matching circuit's adjustment.

3. Experimental results

In order to evaluate the performances achieved by the system developed above, a number of measurements have been performed inside Slanic Prahova Cantacuzino salt mine. The antennas were placed into the salt ~~ore~~ block as shown in Fig. 11.

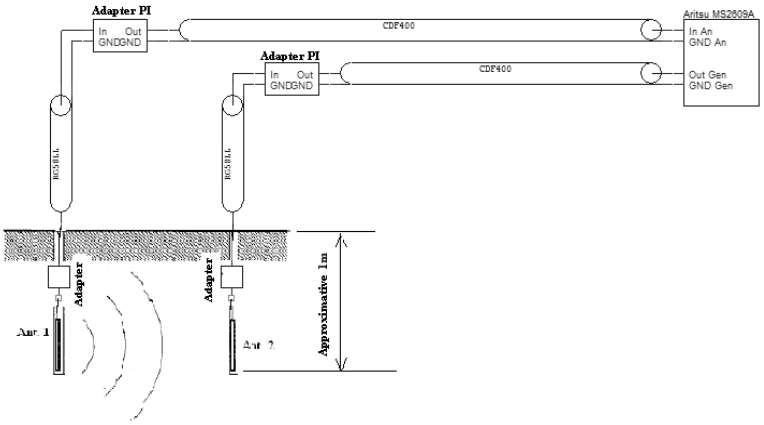

Fig. 11. Experimental positioning of the antennas into the salt mine.

The measurements were made for 495 MHz and 750 MHz frequencies, 7 measurement points, as shown in Fig. 12, were chosen. The holes made for introducing the antennas in salt have 4 cm diameter and had 0.9 m depth. The receiver antenna has been considered fixed (placed in point "0"in Fig. 12) while the transmitter antenna was moved for each measurement in different 7 positions (A1 to A7 in Fig. 12). An example of antenna placement is shown in Fig. 13.

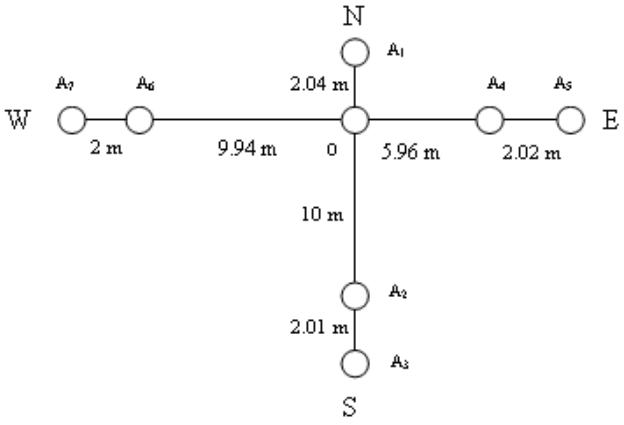

Fig. 12. The measurement points considered during the experimental setup for propagation measurement in salt ore in Slanic Prahova Cantacuzino mine.

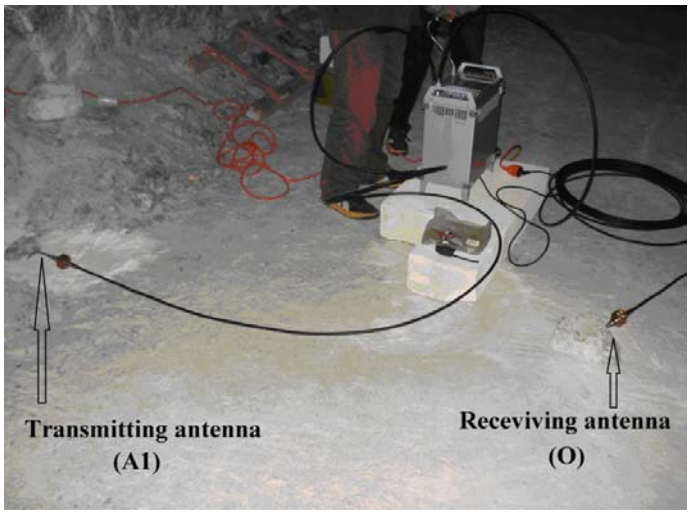

Fig. 13. Example of antennas placement during the measurements campaign of radio-wave propagation through the salt ore.

Based on a number of previous measurements [15], two values have been chosen for the electric permittivity of the salt, namely $\varepsilon_r = 6 + j0.006$ and $\varepsilon_r = 6 + j0.06$. In Figs. 14 and 15 there are shown the simulated values of the absolute value of the electromagnetic field as a function of frequency for the two values of the permittivity [15].

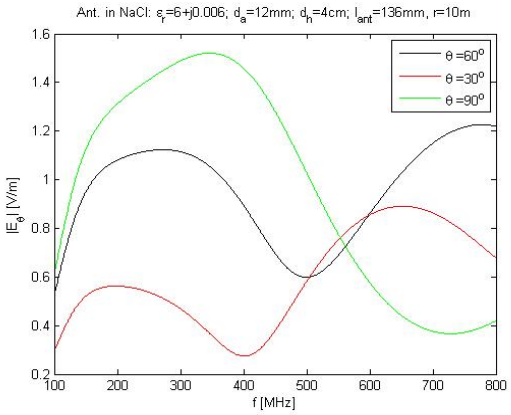

Fig. 14. Electric field generated in salt for a dipole antenna versus frequency for $\varepsilon_r = 6 + j0.006$; the angle θ is considered as parameter.

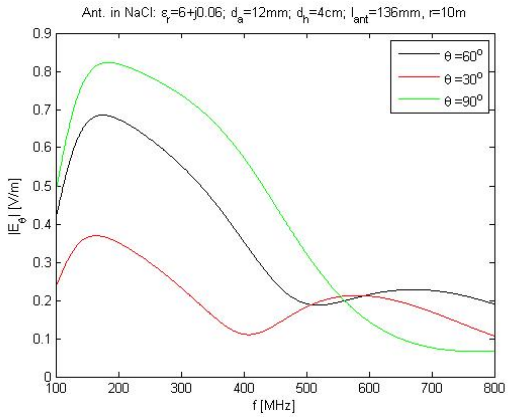

Fig. 15. Electric field generated in salt for a dipole antenna in function to frequency for $\varepsilon_r = 6 + j0.06$, the angle θ is considered as parameter.

Simulations have been performed for an antenna with a diameter d_a=12mm and the length l_{ant}=136mm, placed within a hole with the diameter d_h=4cm; the electromagnetic field is measured at the distance r=10m, while θ is the angle between the propagation direction and the antenna axis.

Comparing Figs. 14 (tg δ = 0.006) and 15 (tg δ = 0.06) we can observe that, for a dipole antenna, the electromagnetic field depends significantly on the loss angle tangent, tgδ. The maximum value of the electromagnetic field being higher as the loss tangent angle is smaller, and occurs at lower frequencies.

Fig. 16 presents the simulated directivity characteristic of the same antenna as a function of the angleθ, for different values of the loss angle tangent (tgδ), at frequency f=495 MHz and Fig. 17 shows the effective length of the antenna as a function of tgδ, for the two working frequencies and different values of θ [15].

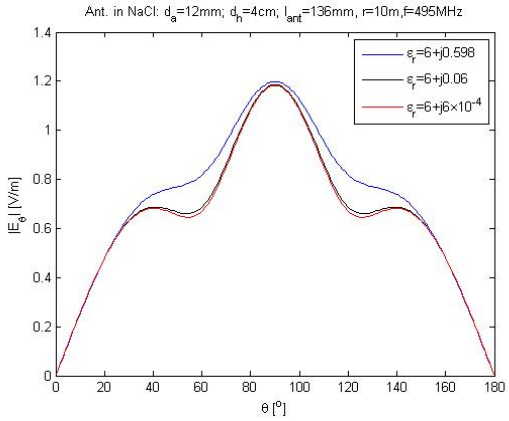

Fig. 16. Directivity characteristic of the antenna with the parameter ε_r.

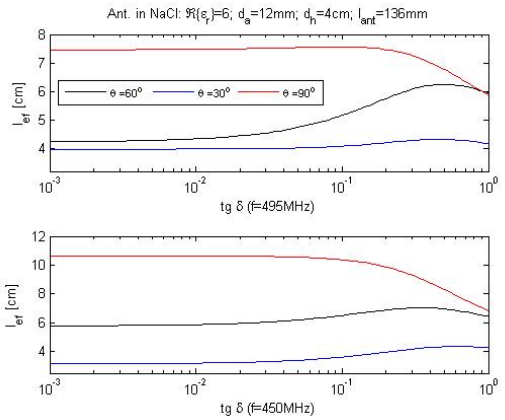

Fig. 17. Effective length of the antenna versus the loss angle tangent (tgδ) for the two frequencies: 450 MHz and 495 MHz.

From those figures we can observe that the effective length of the antenna is approximately constant as of tgδ is smaller then 10^{-1}, and then decreases rapidly.

Fig. 18 shows the noise level was measured in air (upper points) and in salt (lower points) [15]. It can be observed that the noise threshold is around -115 dBm in air while in salt is much lower, around -119 dBm.

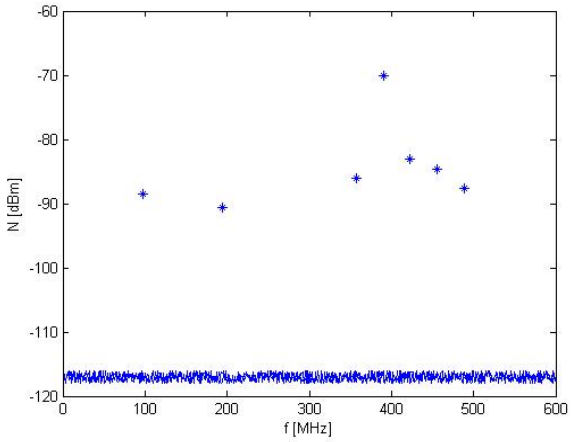

Fig. 18. The measured noise at different working frequencies.

From those simulations we can observe that, by introducing the antenna into the salt block, almost all its parameters (radiation pattern, input impedance, frequency band, the effective length, etc.) changes with respect to the original ones. This is caused by the random distributions of impurities in the salt block.

In order to control and eliminate, if possible, the effects introduced by each element of the measurement chain is necessary to determine the attenuation introduced by each block.

Based on the measurements performed, we determined the antenna feeding cable attenuation, at the two frequencies of interest. The results are shown in Table 1.

In order to determine the attenuation introduced by the two antennas and Π matching circuits, a signal of 1 dBm power level is injected into the circuit. The distance between the two antennas (transmitting/receiving) is 1m. The results are presented in tables 2, 3, 4 and 5.

Table 1

Attenuation introduced by the cables

F	CFD400-E (5m)	R-6763,O400 (21m)
450MHz	-0.31 dBm	-3.05 dBm
750MHz	-0.6 dBm	-4.22 dBm

Table 2

Attenuation introduced by the antenna (L_a = 0.136 m) without matching circuit

f [MHz]	450	440	460
P_{out} [dBm]	-13,2	-14,3	-15,8

Table 3

Attenuation introduced by the antenna (L_a = 0.136 m) with matching circuit

f [MHz]	700	450	490
P_{out} [dBm]	-33	-41,3	-46,4

Table 4

Attenuation introduced by the antenna (L_a = 0.082 m) without matching circuit

f [MHz]	750	740	700	800
P_{out} [dBm]	-22	-22	-25,4	-22,49

Table 5

Attenuation introduced by the antenna (L_a = 0.082 m) with matching circuit

f [MHz]	750	450
P_{out} [dBm]	-33.5	-32.47

4. Conclusions and Future Work

In the context of measurement the electromagnetic field caused by neutrinos passing through dense dielectric medium, like salt, a very sensitive and reliable test-bead has to be implemented. Since the absolute value of the electric field has to be measured, all the instrumental errors have to be exactly evaluated and corrected before the effective measurements are performed. This implies perfect amplitude calibration as well as system delay correction. Since those measurements are independent of external events, there is no need of an absolute

timescale, and, therefore, only the relative time delays between the antennas have to be known.

To eliminate the systematic errors that occur we calculated the differential attenuation, considering two points in the same direction. We have removed the attenuation introduced by the cable and the antenna. The global values given in table 6 have been obtained [15].

Table 6

Attenuation length in the measurement directions (see Fig. 11)

Direction of measurement	*f* [MHz]	S	E	W
Attenuation length [m]	450	3,41	1,01	9,71
	495	1,23	1,92	7,52
	550	2,12	1,47	9,61

We noticed that the lowest frequency is most suitable for further experiments. From table 6 it is clear that the attenuation length depends on the measuring point, due to the irregular distribution of impurities in the salt ore.

On the other hand, the results obtained in table 6 are lower than the expected ones. This can be explained by the fact that the antennas were designed for operating in salt, considering that the propagation media is homogeneous. But, in practice, we have an air cavity around each antenna, which is difficult to be characterized mathematically from radio propagation point of view. There are reflections, refractions and dispersions in the proximity of the antenna and, consequently, additional propagation losses and difficulties of matching the antenna at the given frequency results.

In order to eliminate the near-field effects due to discontinuities of the propagation media, one possibility is to fill up the cavities that remains between the antennas and the salt block with saline solution and let it re-crystallize around the antennas.

It is quite clear that it is very difficult to completely control the conditions in the proximity of the antenna (for example the conductivity of the salt, in case we are using solutions of salt in water to re-crystallize the salt), but a mounting procedure must to be developed in order to obtain better propagation performances.

R E F E R E N C E S

[1] *V. S. Berezinsky, & G. T. Zatsepin*, "Super GZK neutrinos: testing physics beyond the Standard Model", Phys. Lett. 28B, P. 423 (1969); Sov. J. Nucl. Phys. 11, 111 (1970)

[2] *D. Saltzberg, P. Gorham, D. Walz, et al*., "Observation of the Askaryan Effect: Coherent Microwave Emission from Change Asymmetry in High Energy Particle Cascades", Phys. Rev. Lett. 86, P. 2802-2803 (2001)

[3] *R. D. Dagkesamanskii, A. R. Beresnyak, A. V. Kovalenko and I. M. Zheleznyk*, "The upper limit to the EHE neutrino flux from observations of the moon with Kalyazin radio

telescope", International Journal of Modern Physics A, July 2006, Vol. 21, No. supp01: pp. 142-146

[4] *P. W. Gorham, et al.*, "Experimental limit on the cosmic diffuse ultrahigh-energy neutrino flux", Phys. Rev. Lett. 93, 041101 (2004)

[5] *P. W. Gorham, et al.,* "Accelerator Measurements of the Askaryan effect in Rock Salt: A Roadmap Toward Teraton Underground Neutrino Detectors", Phys.Rev. D72 (2005) 023002

[6] *ANITA collaboration: P. W. Gorham, et al.*, "Observations of the Askaryan Effect in Ice", Phys.Rev.Lett.99:171101,2007

[7] *Askaryan GA*, "Radiation Of Volume And Surface Compression Waves During Impingement Of A Nonrelativistic Electron Stream At The Surface Of A Dense Medium", Soviet Physics-Technical Physics 4 (2): 234-235 1959

[8] *Chiyan Luo, Mihai Ibanescu, Steven G. Johnson, and J. D. Joannopoulos*, "Cerenkov Radiation in Photonic Crystals", Science **299**, 368–371 (2003)

[9] *S. R. Coleman and S. L. Glashow*, "Cosmic ray and neutrino tests of special relativity". Phys. Lett. B 405, 249 (1997)

[10] *K. G. Zloshchastiev*, "Vacuum Cherenkov effect in logarithmic nonlinear quantum theory". Phys. Lett. A 375, 2305-2308 (2010)

[11] *A. M. Badescu et al.,* "Radio technique for investigating high energy cosmic neutrinos", Romanian Reports in Physics, Vol. 64, No. 1, P. 281–293, 2012

[12] *Richard Fitzpatrick*, "Classical Electromagnetism: Electromagnetic Radiation, The Hertzian dipole", The University of Texas at Austin, 2006.02.02.

[13] *V. Cehan*, "Bazele radioemițătoarelor", Ed. Matrix Rom, Buc., 1997, ISBN 973 9254-39-X

[14] *Edward B. Rosa,* "The self and mutual inductances of linear conductors", Bulletin of the Bureau of Standards, [Vol. 4, No.2], 301-344, Washington, September, 15, 1907

[15] *A. M. Badescu, V. Savu, O. Fratu,* Measurements in Slanic Prahova Mine, Gap Report IV (DETCOS-82-104/2008), 10 Dec. 2011